G-quadruplex Binding Protein Developed using the RGG Domain in TLS/FUS Inhibits Transcription of c-myc

Luthfi Lulul Ulum
Shizuoka University
Ryota Yagi
Shizuoka University
Tomoe Kawashima
Shizuoka University
Takanori Oyoshi (oyoshi.takanori@shizuoka.ac.jp)
Shizuoka University

Research Article

Keywords: G-quadruplex Binding, RGG Domain, TLS/FUS Inhibits Transcription, c-myc

Posted Date: September 22nd, 2021

DOI: https://doi.org/10.21203/rs.3.rs-917328/v1

G-quadruplex Binding Protein Developed using the RGG Domain in TLS/FUS Inhibits Transcription of *c-myc*

Luthfi Lulul Ulum[b], Ryota Yagi[b], Tomoe Kawashima[b], and Takanori Oyoshi[a,b,*]

[a] Department of Chemistry, Graduate School of Integrated Science and Technology, Shizuoka University, 836 Ohya Suruga, Shizuoka, 422-8529, Japan

[b] Department of Chemistry, Graduate School of Science and Technology, Shizuoka University, 836 Ohya Suruga, Shizuoka, 422-8529, Japan

[*]To whom correspondence should be addressed. Tel: +81-54-238-4760; Fax: +81-54-237-3384; Email: oyoshi.takanori@shizuoka.ac.jp

Abstract

The G-quadruplex structure in the genome is an important drug target because it regulates gene expression and the genome structure. Several small molecules that bind the G-quadruplex have been developed, but few artificial G-quadruplex binding proteins have been reported. We previously reported a novel G-quadruplex DNA binding protein (RGGF) engineered using the Arg-Gly-Gly repeat (RGG) domain of TLS (translocated in liposarcoma). Here we show that RGGF recognizes DNA loops in the G-quadruplex and preferentially binds G-quadruplex DNA with long loops. Furthermore, RGGF binds to G-quadruplex DNA of the *c-myc* promoter *in vitro* and represses *c-myc* transcription *in vivo*. On the basis of these findings, G-quadruplex binding protein engineered from the RGG domain will be useful for investigating G-quadruplex transcriptional function in the genome.

Introduction

G-quadruplexes are noncanonical secondary structures formed in guanine-rich sequences that are involved in important biologic roles in the genome, such as replication, gene expression, genome stability, telomere maintenance, and histone modification.[1,2] The G-quadruplex conformation provides selective DNA and RNA structures targeted by small molecules, and several such molecules have been developed. Functional studies of the G-quadruplex in DNA and RNA using G-quadruplex–binding small molecules revealed that these molecules stabilize G-quadruplexes, and repress the transcriptional and translational activities of promoters and mRNA with G-quadruplexes, respectively.[1,2] Artificial G-quadruplex binding proteins constructed from the G-quadruplex–binding domain of helicase RHAU (also named DHX36 or G4R1) facilitate the detection of the G-quadruplex in DNA and RNA.[3,4] We reported the assembly of G-quadruplex DNA- and RNA-binding proteins from the Arg-Gly-Gly repeat (RGG) domain of TLS (translocated in liposarcoma) protein and FUS (fused in sarcoma) protein, respectively.[5,6] These molecules revealed that telomere DNA and telomeric repeat-containing RNA (TERRA), G-quadruplex DNA and RNA, respectively, promote histone methylation at different amino acid sites in the telomere region. The RGG domain is conserved in several G-quadruplex binding proteins, such as TLS/FUS, Ewing's sarcoma protein (EWS), heterogeneous ribonucleoprotein A1, nucleolin, cold-inducible RNA-binding protein, and fragile X mental retardation protein, but the RGG domain as a molecule to regulate G-quadruplex function has not been well investigated.[7-13] Here, we found that the engineered RGG domain of TLS/FUS containing Phe (RGGF) recognizes the DNA loop in the G-quadruplex and inhibits the transcription of *c-myc*. These

data confirm that the RGG domain is a potentially useful tool for regulating and exploring the function of G-quadruplexes.

Methods

Plasmid Constructs and DNA. For the polymerase chain reaction (PCR) template, we used pGEX-RGG3, which was previously cloned as RGG3 of TLS/FUS into the pGEX6P-1 vector (Cytiva, Tokyo, Japan).[7] pGEX-RGGF was obtained by deletion in pGEX-RGG3 using a KOD-Plus-Mutagenesis Kit (Toyobo, Tokyo, JP). pGEX-RGGF was constructed by PCR using pGEX-RGG3 as the template and the following RGGF primers: forward, d(CGG GGC CGC GGC GGG GAC CG), and reverse, d(GTT ACC CCC CAT GTG AGA GCC ACC). The nucleolin plasmid, which contains the nucleolin RBD-RGG domain (267-710), was constructed as described previously.[20] The FLAG- and GFP-tagged RGGF plasmid (pLPC-FLAG-GFP-RGGF) was constructed by PCR using pGEX-RGGF as the template. pLPC-FLAG-GFP-RGGF was constructed by PCR using pGEX-RGGF as the template with the RGGF forward and reverse primers. All constructs underwent automated DNA sequencing for verification. All oligomers used for plasmid constructs, the EMSA, and circular dichroism spectroscopy were obtained from Operon Biotechnologies (Japan).

Expression and purification of glutathione S-transferase (GST) fusion proteins. For the *in vitro* experiments, the recombinant proteins were fused to the N-terminus of GST, and overexpressed in *Escherichia coli* as previously reported.[6] PreScission protease (8 units/mL, Cytiva) in buffer was used to remove the GST tags from the RGGF, which was then loaded

on a column for 16 h at 4°C and eluted with a potassium-Tris buffer (20 mM Tris-HCl [pH 7.5], 20 mM KCl). The nucleolin GST tags were eluted by adding reduced glutathione and changing the buffer to a potassium buffer by dialysis. Protein concentration was measured using a BCA Protein Assay Kit (Thermo Scientific, Waltham, MA, US). The proteins were all stored at 4°C and used within 12 h of purification.

Electrophoretic Mobility Shift Assay (EMSA). The EMSA and binding affinity measurements were performed as described previously.[6] The ^{32}-P labeled G-quadruplexes were formed by heating the samples with a thermal heating block to 95°C and then cooling them in potassium buffer in 2°C/min steps to 4°C. The binding reactions were conducted in 20 μL (final volume) with 1 nM labeled oligonucleotides with 50 nM protein and 0.1 mg/mL bovine serum albumin in potassium buffer. The competition assay was performed with 1 nM labeled c-MYC with 50 nM nucleolin and 50 nM, 2.5 μM, or 5.0 μM RGGF; and 0.1 mg/mL bovine serum albumin in potassium buffer. The samples were then incubated for 30 min at 4 °C, and then electrophoresed on a 6% polyacrylamide (acrylamide/bisacrylamide = 19:1) nondenaturing gel at 10 V/cm for 100 min at 4 °C. The gel and electrophoresis buffer both contained 0.5x TBE buffer (45 mM Tris base, 45 mM boric acid, and 0.5 mM EDTA) with or without 20 mM KCl. Following electrophoresis, the gels were placed in a phosphorimager cassette and imaged using the Personal Molecular Imager FX (Bio-Rad Laboratories, Hercules, CA, USA). The equilibrium dissociation constants (K_d) were determined by plotting the data from 4 replicate experiments as f (1 fraction of free DNA) versus the protein concentration, which is equivalent to the amount of protein that binds half of the free DNA.

The binding reactions were carried out in a final volume of 20 μL with 1 nM labeled oligonucleotide and various concentrations of purified protein dissolved in a solution of 0.1 mg/mL bovine serum albumin in potassium buffer. The K_d was calculated by nonlinear regression using Microsoft Excel 2011 according to the following equation: $f = [P]/\{K_d + [P]\}$.

Cell Culture and Transfection. Details regarding the cell culture and transfection procedures were described previously.[6] HeLa cells were maintained in Dulbecco's modified Eagle's medium containing 10% fetal bovine serum. For the assays, the HeLa cells were cultured in 6-well plates and transfected with plasmids using Xfect transfection reagent (Takara Bio, Shiga, JP) for protein expression. G418 (200 μg/ml) was added to the culture medium every 3 days.

Western Blot Analysis. Western blot analysis was performed as previously described.[6] Expression of RGGF was confirmed by sodium dodecyl sulfate-polyacrylamide gel electrophoresis using a 12% gel. For visualization of FLAG-tagged proteins, they were transferred to polyvinylidene difluoride membranes and probed using a mouse monoclonal anti-FLAG M2 antibody (MilliporeSigma, St. Louis, MO). Anti-mouse horseradish peroxidase was used as the secondary antibody (Cell Signaling Technology, Danvers, MA, USA). Protein bands were visualized using The ECL Western Blotting Analysis System from GE Healthcare (UK) was used to visualize the protein bands.

Northern Blot Analysis. Total RNA of HeLa cell-transfected plasmids was prepared according to the TRIzol (Gibco-BRL) method as per the manufacturer's instructions. Northern blot transfers were analyzed using *c-myc* and glycerol 3-phosphate dehydrogenase (GAPDH). The ^{32}P-labeled DNA probes were prepared using the BcaBEST Labeling Kit (Takara) with *c-myc* and GAPDHcDNA as per the manufacturer's protocol. Quantification of the *c-myc* and GAPDH expression levels was performed using a Personal Molecular Imager FX (Bio-Rad Laboratories).

Results and Discussion

Previously, we identified that the RGG domain of the C-terminal region (RGG3) of TLS/FUS binds to G-quadruplex DNA and RNA (Figure 1).[7] Nuclear magnetic resonance analysis and electrophoretic mobility shift assays (EMSA) revealed that RGG3 binds the loops and G-tetrads in the G-quadruplex.[5,7,13] Moreover, we reported that RGGF specifically binds to G-quadruplex DNA and inhibits specific histone modifications in telomere region, although the binding mechanism is unclear.[6] To investigate whether RGGF mainly recognizes the loops or G-tetrad of G-quadruplex DNA, we examined the binding of RGGF to ^{32}P-labeled TERRA, human telomere DNA (Htelo), 4 d(GGG) repeat without loops (Oligo 1), or r(UUA) loops (Oligo 2) and 4 r(GGG) repeat with d(TTA) loops (Oligo 3) by EMSA (Figure 2A, Table 1). The purification of all proteins reported herein was confirmed by sodium dodecyl sulfate-polyacrylamide gel electrophoresis (Supplementary Figure S1), and the G-quadruplex structures were confirmed by circular dichroism spectroscopy (Oligo 5; Supplementary Figure S2).[5] The EMSA revealed that the G-quadruplex of Oligo 3 is

favorable for binding, whereas the G-quadruplexes of Oligo 1, TERRA, and Oligo 2 are unfavorable for binding, indicating the preferential binding of RGGF to G-quadruplexes with DNA loops. We next evaluated how the base and ribose in the nucleotide on the loop in the G-quadruplex are singled out by RGGF for binding (Figure 2B, Table 1). On the basis of the EMSA results, RGGF favored binding G-quadruplexes containing 3 DNA abasic loops (Oligo 5), but not G-quadruplexes containing 3 RNA abasic loops (Oligo 4). These observations indicate that RGGF is able to discriminate between DNA and RNA loops in the G-quadruplex.

<Figure 1>

<Table1>

<Figure 2>

We previously reported preferential binding of the RGG3 of EWS, which is functionally related to TLS/FUS as a subgroup of a ribonucleoprotein family, and nucleolin, comprising 4 globular RNA binding domains (RBDs) and an RGG domain, to G-quadruplexes with longer loops.[14,15] Therefore, we evaluated the influence of loop length in G-quadruplex structures on RGGF binding by EMSA (Table 1 and Figure 3). In a previous report, we found that the circular dichroism spectra of G-quadruplex DNA with 4 d(GGG) repeats containing $d(T)_n$ loops (n = 1-3) in the middle loop (L111, L121, and L131) with 2 d(T) segments in the loops are typical of the parallel strand G-quadruplexes in 100-mM KCl and 10-mM Tris-HCl buffer (pH 7.4).[14] An EMSA of RGGF with L111, L121, and L131, and Htelo indicated that the G-quadruplex containing Htelo and L131 was most favorable for binding, and the G-quadruplex containing L111 was the most unfavorable for binding. Moreover, we analyzed the binding activities of RGGF to G-quadruplexes containing $d(T)_n$ loops (n = 1-3) in the two lateral loops (L111, L212, and L313) with d(T) in the central loops (Supplementary Figure

S3), which forms parallel strand G-quadruplexes in 100-mM KCl and 10-mM Tris-HCl buffer (pH 7.4).[14] An EMSA showed that L313 had the best binding to RGGF. These observations suggest that RGGF binds preferentially to G-quadruplex DNA with longer loops. Previously, we reported that RGG domain recognizes the phosphate and the ribose of the loops in G-quadruplex.[5,14] This binding mode might cause the preferential binding of RGGF to G-quadruplex with longer loops.

<Figure 3>

Many G-quadruplex binding small molecules that inhibit *c-myc* transcription have been reported.[16] The DNA oligomer derived from the human *c-myc* promoter (c-MYC) forms an intramolecular propeller-type parallel-strand G-quadruplex in K^+-containing solution.[17] This DNA element transiently forms a G-quadruplex in the genome, which represses transcription.[16] The c-MYC structure contains 3 loops, with the 2 nucleotides in the central loop. Before investigating the effect of RGGF on *c-myc* transcription, an EMSA of RGGF was conducted with various concentrations of c-MYC to analyze the ability of RGGF to bind c-MYC (Table 1 and Figure 4). With an increase in the RGGF concentration, there was a decrease in the amount of free DNA, as well as an increase in the amount of the higher-molecular weight complex. Fitting the mobility shift data to a hyperbolic equation gave a dissociation constant (K_d) of 2.7 ± 0.2 μM. The K_d of RGGF with Htelo was 10 ± 2 nM.[6] Different loop lengths between Htelo and c-MYC might lead to different binding activities of RGGF to G-quadruplexes.

<Figure 4>

Nucleolin is a G-quadruplex binding protein that inhibits the activity of the *c-myc* promoter.[18] The N- and C-terminal ends of the protein contain an acidic region and an RGG

domain, respectively, with RBDs located in the central region. A previous study demonstrated that the RBDs and RGG domain of nucleolin mainly bind to G-quadruplex c-MYC and the filter binding assay data were fitted to a hyperbolic equation, giving a K_d of 103 nM.[19] To investigate whether RGGF affects nucleolin binding to c-MYC, RGGF and truncated nucleolin containing RBDs and the RGG domain were used in competition assays with ^{32}P-labeled c-MYC (Table 1, Figure 5). Lanes 2 and 3 in Figure 5 show that each position of the c-MYC-RGGF and c-MYC–nucleolin complex in the gel was different due to the different molecular weights of RGGF and truncated nucleolin. Adding excess RGGF inhibited the binding of nucleolin to c-MYC (Lane 3-5, Figure 5). Thus, adding excess RGGF competitor inhibited nucleolin binding to c-MYC.

<Figure 5>

To investigate whether RGGF affects the *c-myc* transcription level, we performed Northern blot analysis with FLAG- and green fluorescent protein (GFP)-tagged RGGF in HeLa cells (Figure 6). The RGGF was expressed by a vector and its expression level was detected by Western blot analysis (Figure 6A). Northern blot analysis with a *c-myc* probe showed a decrease in the mRNA density in RGGF-expressing HeLa cells (47.5 ± 5.0%) (Figure 6B). Figure 6C shows quantification of the Northern blot analysis represented by Figure 6B. As a control, a vector that did not express RGGF did not affect the mRNA density of *c-myc*. These findings suggest that RGGF binds to the G-quadruplex of the *c-myc* promoters, thereby repressing its transcription.

<Figure 6>

Conclusion

Here, we demonstrated that RGGF constructed from the RGG domain of TLS/FUS binds to G-quadruplexes having longer DNA loops (Figures 2 and 3). We previously reported that other engineered RGG domains from TLS/FUS and the RGG domain of EWS recognize loops in the G-quadruplex.[5,14] A recent paper reported that nucleolin, which consists of 4 RNA recognition motifs and an RGG domain, preferentially binds to G-quadruplexes with longer loops.[15] Loops in G-quadruplexes are an important common structure recognized by G-quadruplex binding proteins with an RGG domain. Furthermore, the dissociation constant of RGGF and c-MYC was 2.7 ± 0.2 μM, and excess RGGF inhibited the binding of nucleolin to c-MYC *in vitro* (Figures 4 and 5). Nucleolin binds to the 5'-terminal and 3'-terminal single strands containing guanine and loops.[15,20] It might be that RGGF competes with nucleolin to bind c-MYC because both proteins have similar binding mechanisms to G-quadruplex loops. These findings suggest that RGGF is a useful inhibiter of G-quadruplex binding proteins. Moreover, overexpressed RGGF inhibited the transcriptional activity of *c-myc* in HeLa cells (Figure 6). An engineered protein has the potential to regulate gene expression by conjugating functional peptides or proteins to DNA binding proteins.[21,22] RGGF might be a useful tool for regulating transcription and investigating the role of G-quadruplex DNA in the genome.

Data availability

All data generated or analyzed during this study are included in figures of the current manuscript.

References

1. Varshney, D., Spiegel, J., Zyner, K., Tannahill, D. & Balasubramanian, S. The regulation and functions of DNA and RNA G-quadruplexes. *Nat. Rev. Mol. Cell Biol.* **21**, 459-474 (2020).

2. Spiegel, J., Adhikari, S. & Balasubramanian, S. The structure and function of DNA G-quadruplexes. *Trends Chem.* **2**, 123-136 (2020).

3. Zheng, K. W. *et al*. Detection of genomic G-quadruplexes in living cells using a small artificial protein. *Nucleic Acids Res.* **48**, 11706-11720 (2020).

4. Dang, D. T. & Phan, A. T. Development of a ribonuclease containing a G4-specific binding motif for programmable RNA cleavage. *Sci. Rep.* **9**, 7432 (2019).

5. Takahama, K. & Oyoshi, T. Specific binding of modified RGG domain in TLS/FUS to G-quadruplex RNA: Tyrosines in RGG domain recognize 2′-OH of the riboses of loops in G-quadruplex. *J. Am. Chem. Soc.* **135**, 18016-18019 (2013).

6. Takahama, K. *et al*. G-quadruplex DNA- and RNA-specific-binding proteins engineered from the RGG domain of TLS/FUS. *ACS Chem. Biol.* **10**, 2564-2569 (2015).

7. Takahama, K. *et al*. Regulation of telomere length by G-quadruplex telomere DNA- and TERRA-binding protein TLS/FUS. *Chem. Biol.* **20**, 341-350 (2013).

8. Takahama, K., Kino, K., Arai, S., Kurokawa, R. & Oyoshi, T. Identification of Ewing's sarcoma protein as a G-quadruplex DNA- and RNA-binding protein. *FEBS J.* **278**, 988-998 (2011).

9. Ghosh, M. & Singh, M. Structure specific recognition of telomeric repeats containing RNA by the RGG-box of hnRNPA1. *Nucleic Acids Res.* **48**, 4492-4506 (2020).

10. Gonzalez, V., Guo, K., Hurley, L. & Sun, D. Identification and characterization of nucleolin as a c-*myc* G-quadruplex-binding protein. *J. Biol. Chem.* **284**, 23622-23635 (2009).

11. Huang, Z. L. *et al*. Identification of G-quadruplex-binding protein from the exploration of RGG motif/G-quadruplex interactions. *J. Am. Chem. Soc*. **140**, 17945-17955 (2018).

12. Darnell, J. C. *et al*. Fragile X mental retardation protein targets G quartet mRNAs important for neuronal function. *Cell* **107**, 489-499 (2001).

13. Kondo, K. *et al*. Plastic roles of phenylalanine and tyrosine residues of TLS/FUS in complex formation with the G-quadruplexes of telomeric DNA and TERRA. *Sci. Rep*. **8**, 2864 (2018).

14. Takahama, K., Sugimoto, C., Arai, S., Kurokawa, R. & Oyoshi, T. Loop lengths of G-quadruplex structures affect the G-quadruplex DNA binding selectivity of the RGG motif in Ewing's Sarcoma. *Biochemistry* **50**, 5369-5378 (2011).

15. Saha, A. *et al*. Nucleolin discriminates drastically between long-loop and short-loop quadruplexes. *Biochemistry* **59**, 1261-1272 (2020).

16. Chaudhuri, R., Bhattacharya, S., Dash, J. & Bhattacharya, S. Recent update on targeting *c-MYC* G-quadruplexes by small molecules for anticancer therapeutics. *J. Med. Chem*. **64**, 42-70 (2021).

17. Phan, A. T., Modi, Y. S. & Patel, D. J. Propeller-type parallel-stranded G-quadruplexes in the human *c-myc* promoter. *J. Am. Chem. Soc*. **126**, 8710-8716 (2004).

18. Gonzalez, V. & Hurley, L. H. The C-terminus of nucleolin promotes the formation of the c-*MYC* G-quadruplex and inhibits c-*MYC* promoter activity. *Biochemistry* **49**, 9706-9714 (2010).

19. Gonzalez, V., Guo, K., Hurley, L. H. & Sun, D. Identification and characterization of nucleolin as a c-*myc* G-quadruplex-binding protein. *J. Biol. Chem*. **284**, 23622-23635 (2009).

20. Masuzawa, T. & Oyoshi, T. Roles of the RGG domain and RNA recognition motif of nucleolin in G-quadruplex stabilization. *ACS Omega* **5**, 5202-5208 (2020).

21. Bae, K. H. *et al*. Human zinc fingers as building blocks in the construction of artificial transcription factors. *Nat. Biotechnol*. **21**, 275-280 (2003).

22. Nishihara, M., Kanda, G. N., Suzauki, T., Yamakado, S., Harashima, H. & Kamiya, H. Enhanced transgene expression by plasmid-specific recruitment of histone acetyltransferase. *J. Biosci. Bioeng*. **123**, 277-280 (2017).

Acknowledgements

This work was partially supported by a Grant-in-Aid for Scientific Research (C) (17K05930) from MEXT, Japan. We thank Dr. George R. Stark at Case Comprehensive Cancer Center at Case Western Reserve University for the *c-myc* cDNA and Dr. Riki Kurokawa at Saitama Medical University Research Center for Genomic Medicine for the GAPDH cDNA.

Author contributions

T.O. conceived the study. R.Y., T.K. and L.L.U. prepared the protein and performed the EMSA assay, Western Blot analysis and Northern Blot analysis. T.O., R.Y., T.K. and L.L.U. analyzed the data and wrote the manuscript.

Competing interests

The authors declare no competing interests.

Additional information

Supplementary Information The online version contains supplementary material available at XXX.

Correspondence and requests for materials should be addressed to T. O.

Table 1.

Oligonucleolide sequences used in EMSA.

Figure Legends

Figure 1. Schematic illustration of TLS/FUS, RGG3, and RGGF. SYQG-rich; RGG 1, Arg-Gly-Gly-rich motif 1; RRM, RNA recognition motif; RGG 2, Arg-Gly-Gly-rich motif 2; ZnF, zinc finger; RGG 3, Arg-Gly-Gly-rich motif 3.

Figure 2. RGGF selectively binds the DNA or RNA loops on the G-quadruplex. EMSA was performed with RGGF and ^{32}P-labeled (A) Htelo, TERRA, or Oligo 1-3; (B) Htelo, TERRA, Oligo 4, or Oligo 5. Gray and red in the cartoon show DNA and RNA, respectively.

Figure 3. Effect of G-quadruplex loop length on the binding affinity of RGGF. The EMSA was performed using RGGF (lanes 2, 4, 6, and 8) with ^{32}P-labeled Htelo (lanes 1 and 2), L131 (lanes 3 and 4), L121 (lanes 5 and 6), or L111 (lanes 7 and 8). The DNA-protein complexes were resolved by 6% polyacrylamide gel electrophoresis and visualized by autoradiography.

Figure 4. Binding activity of RGGF to G-quadruplex c-MYC. The equilibrium binding curve was obtained by calculating the fraction of ^{32}P-labeled c-MYC at varying RGGF concentrations. The dissociation constant (K_d) was ascertained by fitting the data to the appropriate equation. The DNA-protein complexes were resolved by 6% polyacrylamide gel electrophoresis and visualized by autoradiography.

Figure 5. Competitive binding of c-MYC to nucleolin and RGGF. EMSA of ^{32}P-labeled c-MYC with nucleolin and RGGF was performed by 6% polyacrylamide gel electrophoresis and visualized by autoradiography. Labeled c-MYC and RGGF (lane 2) or nucleolin (lane 3) were incubated and analyzed as a control. A competitive binding assay of ^{32}P-labeled c-MYC to nucleolin was performed in the presence of RGGF at the indicated molar ratios (lanes 4-6).

Figure 6. Transcription level changes in *c-myc* in RGGF-overexpressing HeLa cells. (A) Overexpressed RGGF was analyzed by Western blot with a FLAG antibody. (B, C) The mRNA levels of *c-myc* and GAPDH were analyzed with Northern blotting and quantified. Bars represent mean values (± errors) obtained from 3 independent experiments.

Figures

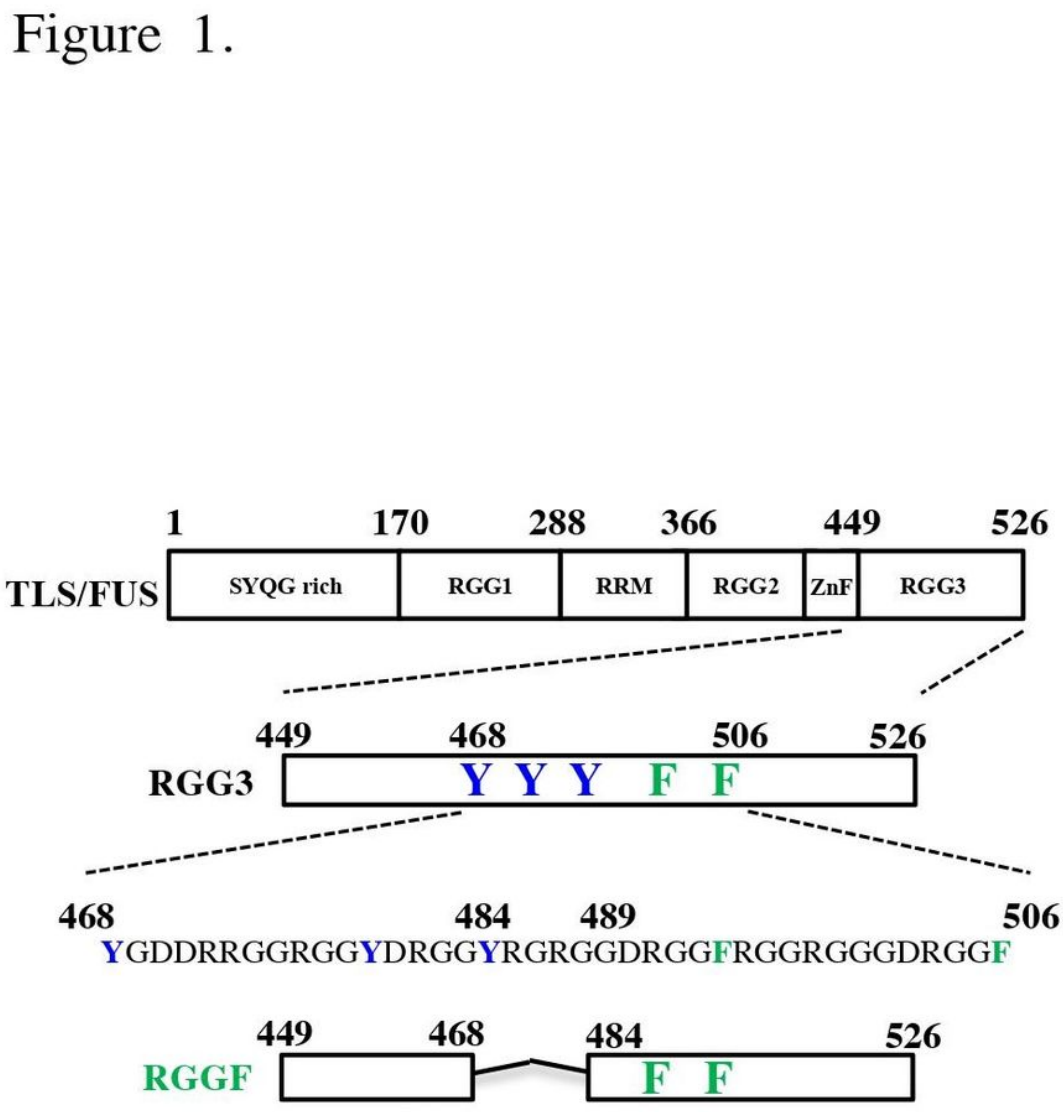

Figure 1

Schematic illustration of TLS/FUS, RGG3, and RGGF. SYQG-rich; RGG 1, Arg-Gly-Gly-rich motif 1; RRM, RNA recognition motif; RGG 2, Arg-Gly-Gly-rich motif 2; ZnF, zinc finger; RGG 3, Arg-Gly-Gly-rich motif 3.

Figure 2.

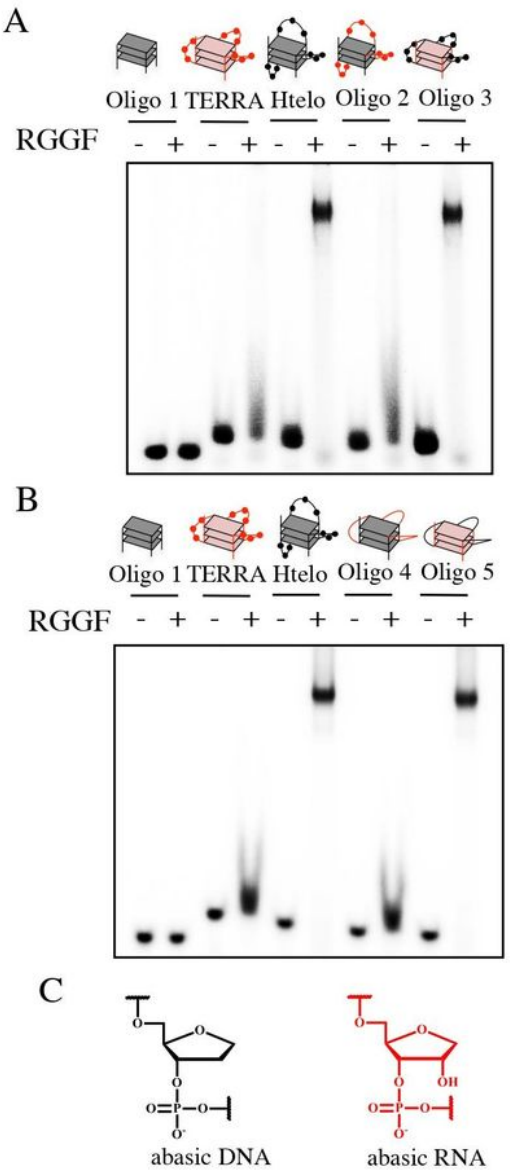

Figure 2

RGGF selectively binds the DNA or RNA loops on the G-quadruplex. EMSA was performed with RGGF and 32P-labeled (A) Htelo, TERRA, or Oligo 1-3; (B) Htelo, TERRA, Oligo 4, or Oligo 5. Gray and red in the cartoon show DNA and RNA, respectively.

Figure 3.

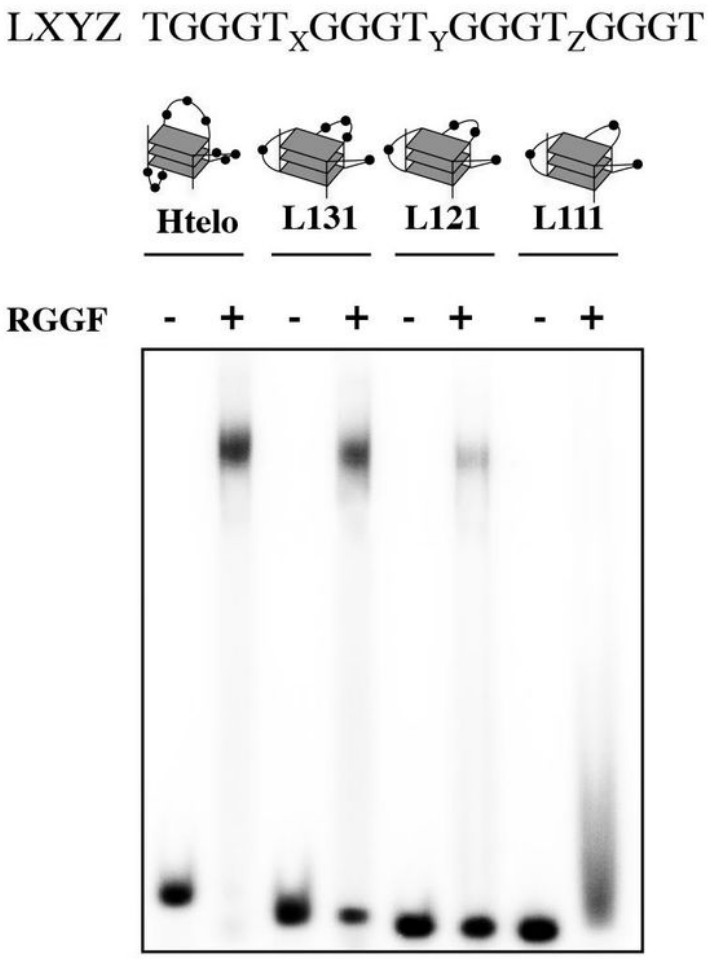

Figure 3

Effect of G-quadruplex loop length on the binding affinity of RGGF. The EMSA was performed using RGGF (lanes 2, 4, 6, and 8) with 32P-labeled Htelo (lanes 1 and 2), L131 (lanes 3 and 4), L121 (lanes 5 and 6), or L111 (lanes 7 and 8). The DNA-protein complexes were resolved by 6% polyacrylamide gel electrophoresis and visualized by autoradiography.

Figure 4.

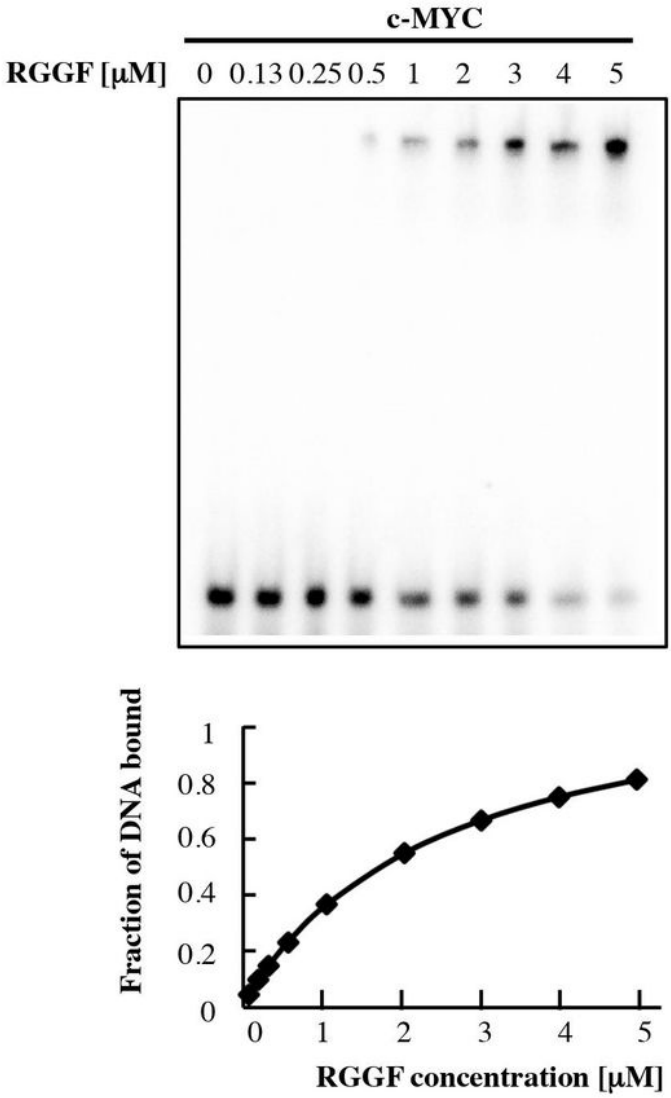

Figure 4

Binding activity of RGGF to G-quadruplex c-MYC. The equilibrium binding curve was obtained by calculating the fraction of 32P-labeled c-MYC at varying RGGF concentrations. The dissociation constant (Kd) was ascertained by fitting the data to the appropriate equation. The DNA-protein complexes were resolved by 6% polyacrylamide gel electrophoresis and visualized by autoradiography.

Figure 5.

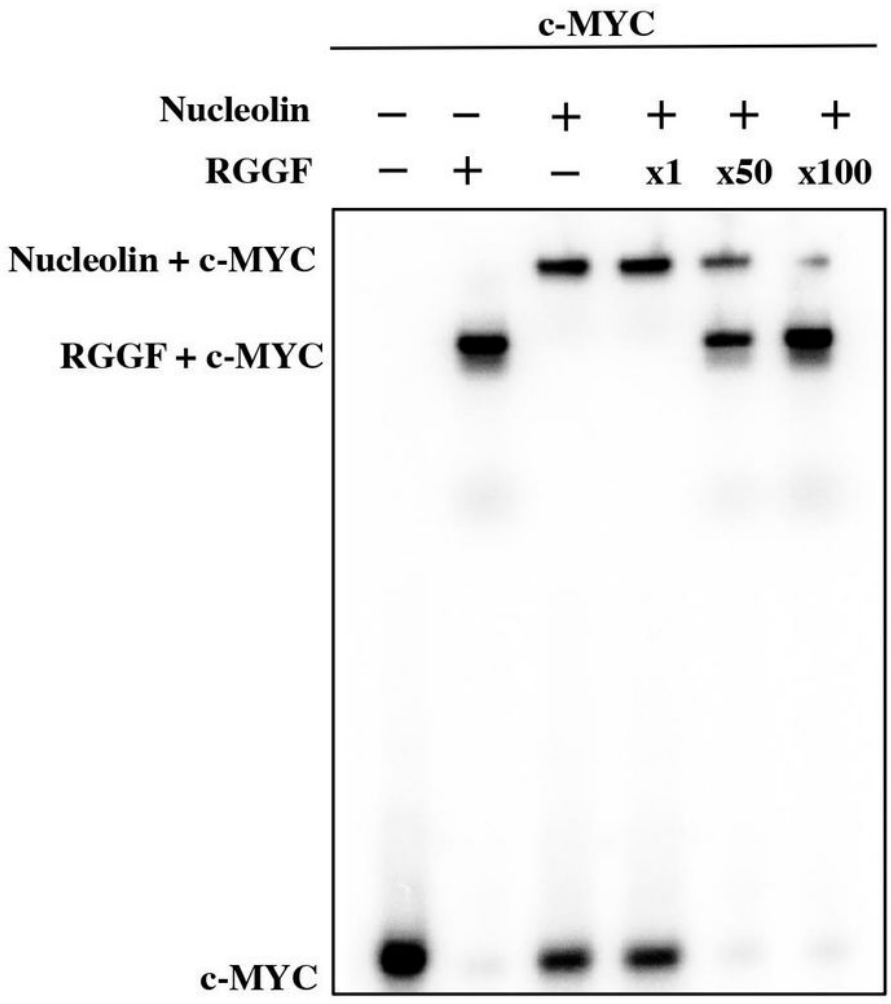

Figure 5

Competitive binding of c-MYC to nucleolin and RGGF. EMSA of 32P-labeled c-MYC with nucleolin and RGGF was performed by 6% polyacrylamide gel electrophoresis and visualized by autoradiography. Labeled c-MYC and RGGF (lane 2) or nucleolin (lane 3) were incubated and analyzed as a control. A competitive binding assay of 32P-labeled c-MYC to nucleolin was performed in the presence of RGGF at the indicated molar ratios (lanes 4-6).

FIGURE 6.

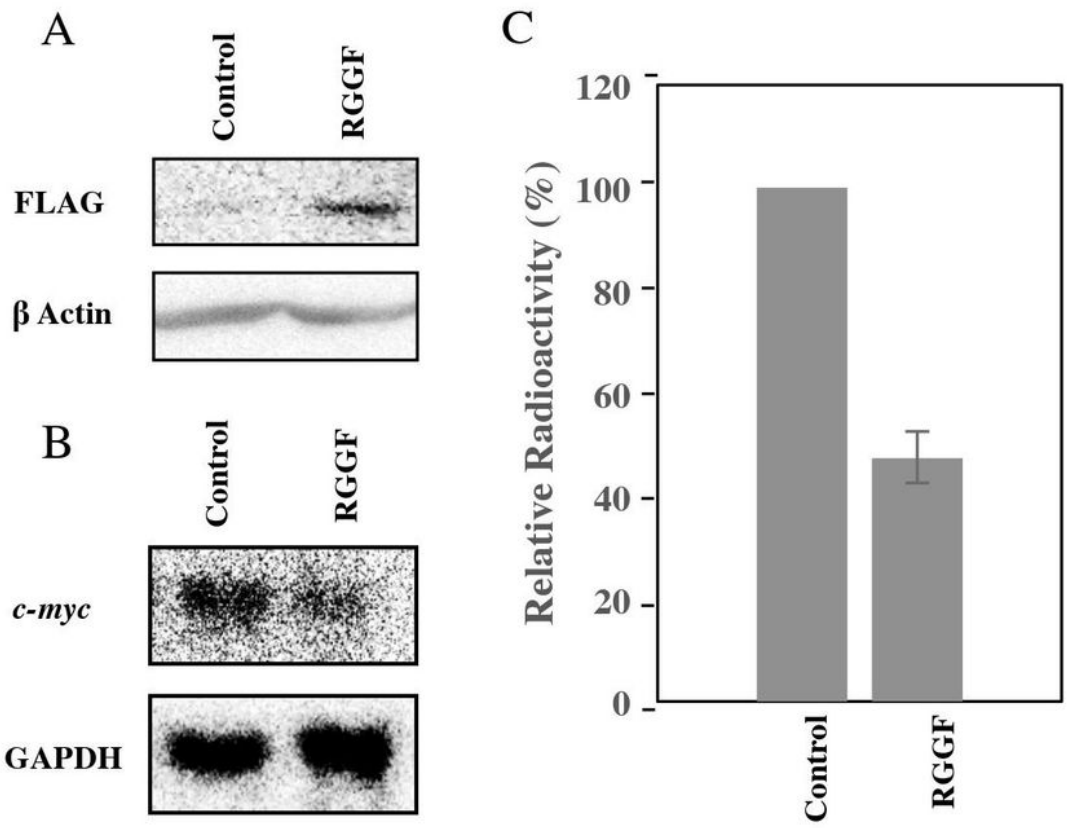

Figure 6

Transcription level changes in c-myc in RGGF-overexpressing HeLa cells. (A) Overexpressed RGGF was analyzed by Western blot with a FLAG antibody. (B, C) The mRNA levels of c-myc and GAPDH were analyzed with Northern blotting and quantified. Bars represent mean values (± errors) obtained from 3 independent experiments

Supplementary Files

This is a list of supplementary files associated with this preprint. Click to download.

- ScientificreportsSI.pdf
- ScientificreportsTable.pdf